SCIENTIFIC PAPERS
OF THE UNIVERSITY OF PARDUBICE
Series A
Faculty of Chemical Technology
6 (2000)

INFLUENCE OF TWO-PHASE GAS-LIQUID FLOW ON PERMEATE FLUX AND CAKE CHARACTERISTICS IN CERAMIC MEMBRANE CROSSFLOW MICROFILTRATION

Petr MIKULÁŠEK[1] and Petr POSPÍŠIL
Department of Chemical Engineering, University of Pardubice
CZ–532 10 Pardubice

Received June 1, 2000

Dedicated to the 50th anniversary of university education in Pardubice

The convection promotion within an aluminium oxide tubular membrane using the gas-liquid two-phase flow was studied for microfiltration of aqueous titanium dioxide dispersions. The influence of gas flow velocity and that of periodical gas flow is also presented.

The results of experiments show that a constant gas-liquid two-phase flow has a positive impact on the flux. From analysis of experimental results it may be concluded that two-phase flow seems to expand the particle cake as it increases both cake porosity and thickness, thus allowing higher fluxes. For the periodical gas flow it was found that the improvement of the permeate flux is less. However, this phenomenon depends on the periodical gas flow mode and on the

[1] To whom correspondence should be addressed.

concentration of the dispersion used.

The most important consideration is that for all the concentrations in the range tested, an enhancement of the permeate flux because of the air injection is always observed. There is no concentration for which air injection has no effect on the permeate flux.

Introduction

The most common cross-flow membrane processes include microfiltration, ultrafiltration, nanofiltration, and reverse osmosis. Although differing in transmembrane pressure difference driving force and average pore diameter, each membrane serves as a selective barrier by permitting certain components of a mixture to pass through while retaining others. This produces two phases, permeate and retained phases, each of which is enriched in one or more of the components of the mixture.

However, the present cross-flow membrane processes for liquid feed streams are still complicated by the phenomena of membrane fouling and of concentration polarisation in the liquid boundary layer adjacent to the membrane wall. Concentration polarisation and membrane fouling are major concerns in the successful use of a membrane-based separation operation, as their net effect is to reduce the permeate flux, thereby resulting in loss of productivity. Therefore, there is a tremendous potential to reduce or control concentration polarisation and fouling in membrane processes and hence alleviate these limitations. Changes in membrane properties, or the feed solution, or the development of concentration polarisation frequently masks the flux decline due to membrane fouling. The concentration polarisation results in a localised increase in the solute concentration on or near the membrane surface. This solute build-up lowers the flux due to an increase in hydrodynamic resistance in the mass boundary layer and due to an increase in local osmotic pressure resulting in a decreased net driving force. However, concentration polarisation effects are reversible, since decreasing the transmembrane pressure or lowering the feed concentration can reduce them. Fouling effects, on the other hand, are usually characterised by an irreversible decline in the flux. Although neither concentration polarisation nor membrane fouling can generally be avoided in membrane separations, there are several possible approaches to reduction or control of their extent. In the past, a number of investigators attempted manipulation of fluid hydrodynamics or membrane surface morphology to enhance the permeate flux. There are at least three possible approaches to reduction or control of concentration polarisation and fouling:

1) Changes in surface characteristics of the membrane,
2) pre-treatment of the feed and,
3) fluid management methods.

In Ref. [1], a morphological analysis of means of reducing concentration polarisation and fouling is presented. Out of the various methods mentioned in Ref. [1], hydrodynamic or fluid management techniques have proved to be quite effective and economical in reducing concentration polarisation and fouling. Recently, some studies have pointed out interest in the area of use of gas-liquid two-phase flow technique in the concentrate stream during ultrafiltration in order to enhance the flux for different applications (biological treatment, drinking water production, macromolecules separation) and different membrane geometries (hollow fibre, flat sheet or tubular).

Application of gas-liquid two-phase flow for microfiltration intensification is based on a change of hydrodynamic conditions inside the microfiltration module, which positively increases the wall shear stress, preventing the membrane fouling and enhancing the mass transfer of the separated compound (solvent, most frequently water).

Cui *et al.* [2–4] have shown that injecting air can reduce the concentration polarisation in ultrafiltration of macromolecules (dextran, dyed dextran and bovine serum albumin) in the case of flat sheet modules and hollow fibre membranes. The explanation given for the flux enhancement is that air sparging into the liquid stream increases turbulence near the membrane surface as well as the cross-flow velocity, thus limiting the boundary layer thickness.

Mercier *et al.* [5,6] obtained significant flux enhancement (200% of flux increase) by air sparging in ultrafiltration tubular inorganic membranes with two kinds of suspension (bentonite and yeast).

Cabassud *et al.* [7,8] have presented results concerning two-phase gas-liquid flow for particle suspensions (clay suspensions) inside hollow fibres. In that case, flux improvement was linked to hydrodynamic control of the particle deposition on the membrane. Significant increases in permeate flux have been observed, even at a very low air velocity, for all the concentrations studied. The air injection process leads to an increase of up to 155% at specific conditions. However, good results have been obtained for very low air velocities (under 0.2 $m\,s^{-1}$).

Lee *et al.* [9] used air slugs entrapped in cross-flow stream to prevent the flux decline during filtration of bacterial cell suspensions. Ultrafiltration and microfiltration flat sheet membranes have been used and the best performance was obtained for the ultrafiltration (maximum enhancement of 200% is reported).

The aim of this study is to determine which operating parameters are involved in flux enhancement and to establish a link between hydrodynamics parameters and cake resistance or structural characteristics (thickness, porosity and specific resistance). Two complementary studies were required: a characterisation of cake properties as a function of filtering parameters and a hydrodynamic study aiming at characterization of the gas flow inside the membrane.

Theory

The effect of time-dependent decreases in permeate flux on the average permeate flux over an operating time, t, can be approximated using a procedure in which the steady-state model for cross-flow filtration is combined with a transient model for dead-end batch filtration. This procedure has been shown [10] to yield a very good approximation to the exact solution for time variable permeate flux J.

The following expression for the time-dependent permeate flux is given [10]

$$J = \frac{J_0}{\left(1 + \frac{2t}{\tau_{cr}}\right)^{1/2}} \tag{1}$$

where

$$\tau_{cr} = \frac{R_m(\varphi_{max} - \varphi)}{J_0 r \varphi} \tag{2}$$

is the time constant associated with the flux decline.
The resistance of the cake layer, r, is estimated using the Blake–Kozeny correlation [11]

$$r = \frac{37.5\varphi_{max}^2}{a^2(1 - \varphi_{max})^3} \tag{3}$$

The volume fraction of the maximally packed particles in the cake layer, φ_{max}, was not measured directly, but a reasonable estimate [12] is given by $\varphi_{max} = 0.65$.

The approximate procedure to predict the total behaviour of the permeate flux, from time zero to steady state, is to use Eq. (1) from dead-end batch filtration until the time the steady state is reached. The underlying reason behind this solution is that, while the cake is initially developing, the effect of the shear rate is small and can be neglected over short times so that cross-flow filtration theory can be effectively approximated by dead-end filtration theory. Nearing the steady state, however, the shear rate begins to arrest the cake growth in cross-flow filtration while dead-end flux profile continues to decline with time. The approximate time to steady-state, t_{ss}, is determined by substituting the steady-state flux, J_s, in Eq. (1)

$$t_{ss} = \frac{1}{2}\left[\left(\frac{J_0}{J_s}\right)^2 - 1\right]\tau_{cr} \tag{4}$$

The characteristics of permeate flux decline, and the associated operating time required to achieve the steady state flux varies as a function of the concentration of dispersions and operating parameters.

The influence of two-phase flow on cake structure then could be analysed. The cake parameters to be determined are specific resistance, porosity and cake thickness.

The cake specific resistance α is linked to the slope of the curve t/V versus V

$$\frac{t}{V(t)} = K_1 V(t) + K_2 \tag{5}$$

where

$$K_1 = \frac{\mu_l \alpha c}{2\Delta P S^2} \tag{6}$$

and

$$K_2 = \frac{\mu_l R_m}{\Delta P S} \tag{7}$$

K_1 and K_2 are constant during constant-pressure separation. The slope K_1 depends on transmembrane pressure difference and properties of the cake; the intercept K_2 also depends on transmembrane pressure difference but is independent of cake properties. The mass of solids deposited per volume of permeate, c, is for low concentrations related to the concentration of solid in the feed.

The particle deposit permeability can be calculated using the Carman–Kozeny equation, when the particle shape and deposit porosity is known

$$k = \frac{1}{K}\frac{\varepsilon^3}{(1-\varepsilon)^2}\frac{1}{a_0^2} \tag{8}$$

The permeability, k, is related to the cake specific resistance, α

$$k = \frac{1}{\alpha\rho_s(1-\varepsilon)} \tag{9}$$

From Eqs (8) and (9) the following expression is obtained

$$\alpha = \frac{K(1-\varepsilon)a_0^2}{\varepsilon^3\rho_s} \tag{10}$$

Using Eqs (6) and (10) the cake porosity, ε, can be obtained from

$$K(1-\varepsilon)a_0^2\mu_l c - 2K_1\Delta P S^2\varepsilon^3\rho_s = 0 \tag{11}$$

This leads to the deposit thickness, δ, given by

$$\delta = \frac{V(t)c}{S\rho_s(1-\varepsilon)} \tag{12}$$

Experimental

Membranes

The membranes used in the experiments with two-phase gas-liquid flow were asymmetric multi-layered ceramic membranes (Terronic a.s, Hradec Králové, Czech Republic). They were configured as a single cylindrical tube 0.1 m long, 6 mm ID and 10 mm OD, consisting of a thin alumina layer deposited on the internal surface of the alumina support. In our experiments, the microfiltration membranes were used with the mean diameter equal to 91 nm. The pore size distribution of the membrane used was determined by the liquid displacement method [13]. A new membrane was

used in each experiment, and before the run the pure water flux was measured with deionised water.

Feeds

The microfiltration experiments were performed with an aqueous dispersion of titanium dioxide (Versanyl B-K7020) obtained from Ostacolor a.s., Pardubice, Czech Republic. The mean diameter of particles was 443 nm; however, the distribution of particles was very wide. Concentration of solids in the dispersion was 1 and 5 % wt during constant concentration experiments. However, during concentration experiments the concentration of solids in the dispersions varied up to 18 % wt.

Equipment

The two-phase gas-liquid experimental apparatus used is shown schematically in Fig. 1. The circulating loop was constructed of stainless steel and contained a five-litre retentate container, a diaphragm pump, the membrane module and a flow control valve at the module outlet. The loop was also equipped with a thermal regulating system, and a pressure, temperature and flow monitoring systems. The velocity and pressure in the retentate loop were varied independently by means of pump controller and an appropriate needle valve. Air was added to the liquid stream at the inlet of the membrane, through a capillary. The airflow rates were controlled by means of a flowmeter.

Procedure

After the membrane was placed in the membrane module, distilled water was circulated in the test loop at the moderate operating pressure for about 2 hours. During this time a stabilisation of the membrane was observed giving relatively stable water permeability. A concentrate of feed substance was then introduced to the unit, preheated to the desired temperature (25 °C), and the operating pressure as well as retentate velocity were adjusted by the regulation system.

The flux through membrane was measured by weighing the permeate and timing the collection period (by use of a balance interfaced with a computer). Both the retentate and permeate were recirculated back into the retentate container. Therefore, the concentration in the recirculation loop remained virtually constant. After each set of experiments the circuit and membrane were rinsed with water and the pure water flux was measured again under the conditions of initial testing until

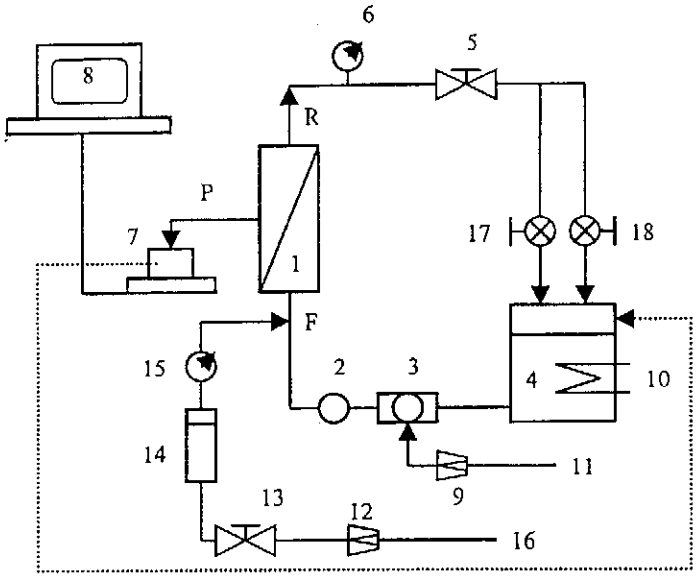

Fig. 1 Set-up of two-phase gas-liquid flow experimental apparatus:1 – microfiltration module; 2 – damper; 3 – pump; 4 – storage tank; 5 – regulating valve; 6 – pressure gauge; 7 – electronic balance; 8 – computer; 9 – pump regulating valve; 10 – thermal regulating system; 11 – air inlet; 12 – air regulating valve; 13 – air valve; 14 – flow gauge; 15 – pressure gauge; 16 – air inlet; 17 – by-pass cock; 18 – closing cock; F – feed; P – permeate; R – retentate

the steady state was obtained. The differences in the steady state pure water flux were taken as a measure of the fouling tendency of the membrane.

Results and Discussion

Two-phase Gas-liquid Flow

The direct observations through the transparent tubular pipe (of the same internal diameter as the membranes) confirmed the published results [14]. Each flow pattern corresponded to values of the superficial gas velocity, u_G, and the superficial liquid velocity, u, respectively, both of them being calculated as each phase was separately circulating. The main structures, which were observed when the gas velocity was increased for a given liquid velocity, included the bubble flow, slug flow, churn flow and annular flow (Fig. 2).

For $u_G = 0.25 - 1.25$ m s^{-1}, large bubbles were observed with a size of the order of the internal diameter of the tube. These bubbles are usually called Taylor bubbles. Due to reduction in the available cross-section for the liquid phase, a thin liquid film always remained over the surface of the membrane and moved in the

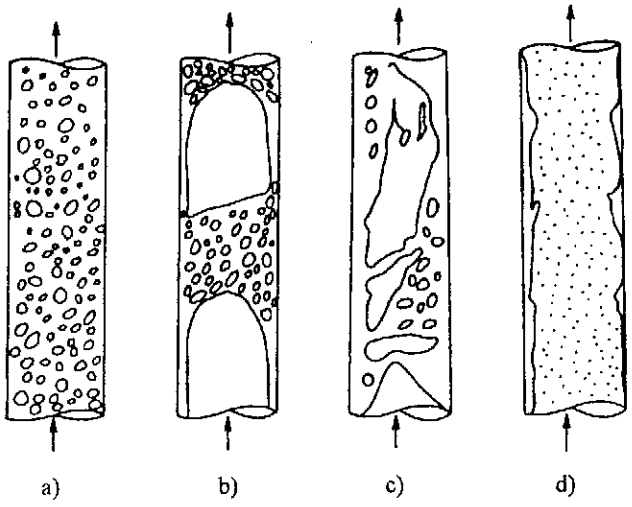

Fig. 2 Two-phase flow patterns in vertical tubes: a) bubble flow; b) slug flow; c) churn flow; d) annular flow

opposite direction with respect to the main flow. This phenomenon induces a highly variable large shear rate against the pipe wall. It should be noted that for a given liquid flow-rate, the presence of the gas increases the mean longitudinal velocity of the fluid which, in association with the great variations in the wall shear stress and the turbulence existing in the churn flow (u_G = 1.5 – 2.3 m s^{-1}), can improve the performance. Previous work showed that slug flow is the most efficient regime for significant enhancement of mass transfer [14].

Effect of Gas Velocity

The effects of gas-liquid two-phase flow on permeate flux were measured. In the range of the experimental conditions (liquid flow velocity 1 m s^{-1} and trans-membrane pressure difference 100 kPa), the permeate flux obtained with gas flow was always larger than at the single-liquid conditions.

Figure 3 shows the results of experiments realised with and without two-phase flow in the feed stream. As generally is the case in cross-flow microfiltration, the permeate flux without injecting air in the feed stream decreases with time. During the first few minutes the flux decreases sharply, due to particle deposit formation which constitutes an additional flow resistance. Then the flux seems to level off. The deposit behaves like a second membrane, with a constant flow resistance with time.

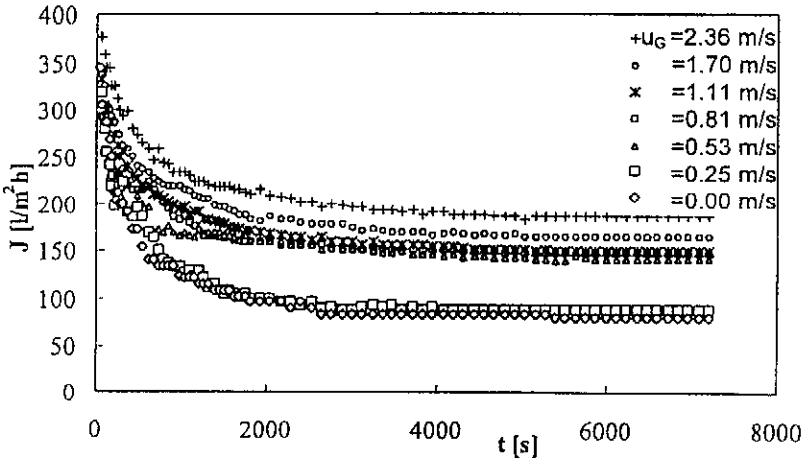

Fig. 3 Influence of gas-liquid flow on microfiltration of dispersions: u = 1 m s^{-1}, ΔP = 100 kPa, x' = 0.01

In the experiments using two-phase flow, air is injected throughout the filtering period. Here, there is also an initial flux decline but less important than the one observed without air. When the gas velocity is higher, the flux is maintained at a higher level during the filtering period as shown in Fig. 3.

The values of the normalised permeate flux as a function of air velocity are plotted in Fig. 4. The normalised permeate flux first increases with the air velocity until it reaches a limit corresponding to u_G = 0.8 m s^{-1}. That is to say that a further increase in air velocity does not result in any significant improvement in the permeate flux. Moreover, it is interesting to notice that even at a relatively low velocity, the two-phase flow can enhance the flux (increase of 70% for a gas velocity of 0.5 m s^{-1}, flux multiplied by 1.7).

Figure 5 represents the evolution of the permeate flux vs. time for u_G = 0, and for u_G = 0.8 m s^{-1} for a steady and a periodical gas flow mode. The periodical gas flow mode consists in stopping air injection for 10 min every 30 min.

The first thing is that even for the periodical gas flow mode, the flux after 1.5 h is increased in comparison with the flux without air. But after each interruption, the permeate flux decreases sharply. Within the first minutes of airflow interruption, a particle deposit is created on the membrane surface which is difficult to remove when the air injection is restored. Then after filtering for 1.5 h the flux reaches 170 l m^{-2} h^{-1} with a steady gas flow, whereas with the periodical gas flow mode it barely amounts to 90 l m^{-2} h^{-1}. The aim of each process is different: the steady process permits to prevent a cake deposit, whereas in the periodical gas flow mode air has to eliminate the deposit built up during the air flow interruption. At similar experimental operating conditions, a steady injecting process is more efficient than

a periodical one, for which higher air velocities may be necessary to sweep the deposit.

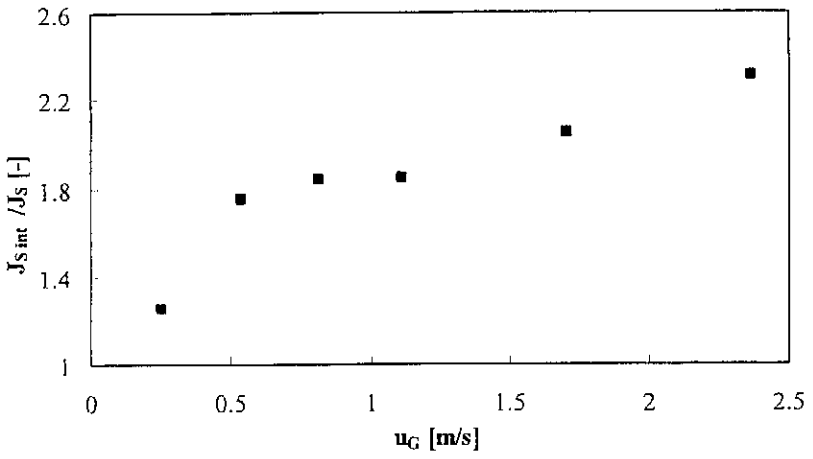

Fig. 4 Influence of gas flow velocity on normalised steady state permeate flux : u = 1 m s^{-1}, ΔP = 100 kPa, x' = 0.01

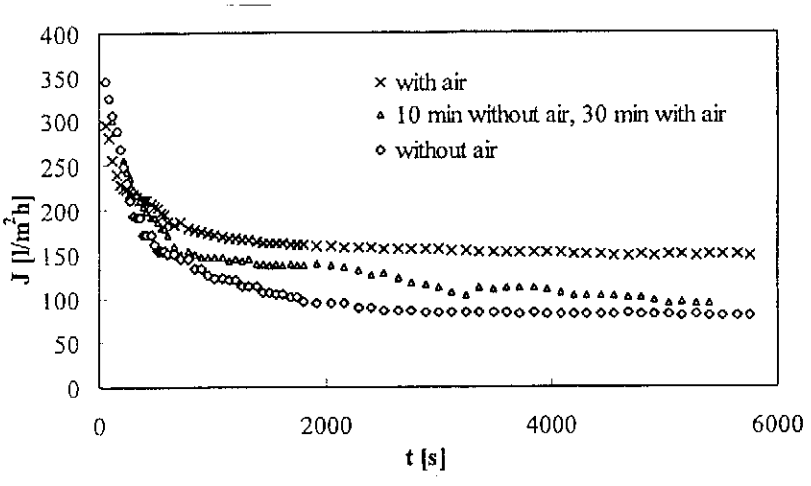

Fig. 5 Influence of a periodical gas flow mode on the permeate flux : u = 1 m s^{-1}, u_G = 0.8 m s^{-1} ΔP = 100 kPa, x' = 0.01

Influence of Gas Velocity on Cake Structure

Figure 6 shows the evolution of cake porosity, ε, with gas velocity for a transmembrane pressure difference 100 kPa and liquid velocity 1 m s^{-1}. The cake porosity increases as air is injected, and can reach nearly 0.55. In the presence of air, the particle cake is very porous. No improvement in porosity is obtained below u_G = 0.5 m s^{-1}.

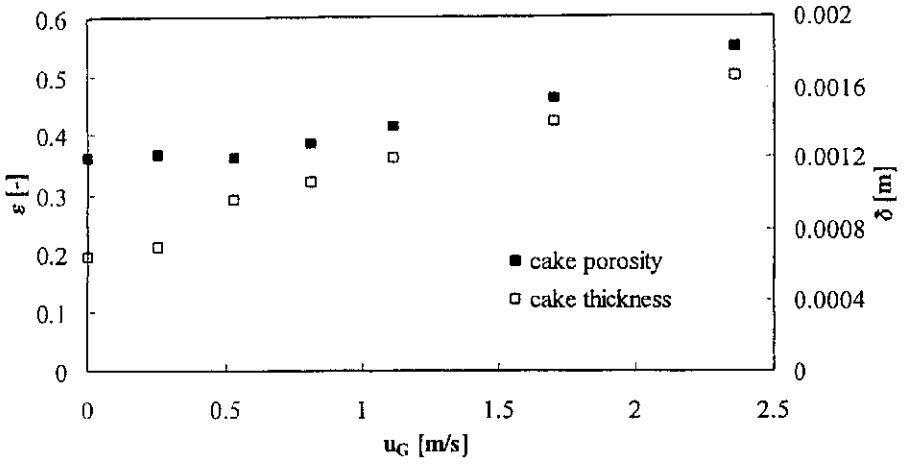

Fig. 6 Influence of gas flow velocity on cake porosity and cake thickness: u = 1 m s^{-1}, ΔP = 100 kPa, x' = 0.01

Furthermore, the cake thickness also increases with air injection, as shown in Fig. 6. The cake thickness is nearly 700 μm without air injection. When two-phase flow is used, it can reach nearly 1600 μm, for a gas velocity around 2 m s^{-1}. The thickness estimated was in agreement with visual observation of the filter cake after microfiltration.

These results show that air injection seems to expand the particle cake: the cake obtained is thicker but more porous than without air, and thus allows higher permeation fluxes.

Effect of Particle Concentration

A more extensive study of the effect of the concentration of the dispersion on permeate flux was undertaken by comparing the conventional single-phase cross-flow microfiltration with two-phase flow membrane system. Figure 7 represents the relationship between the solids mass fraction of the dispersions and the permeate

flux for three systems tested. This relationship depends on the flow mode. For $u_G = 0$, the flux decreases sharply with concentration. This decrease may be related to the cake layer behaviour: the particle deposit becomes denser and less permeable.

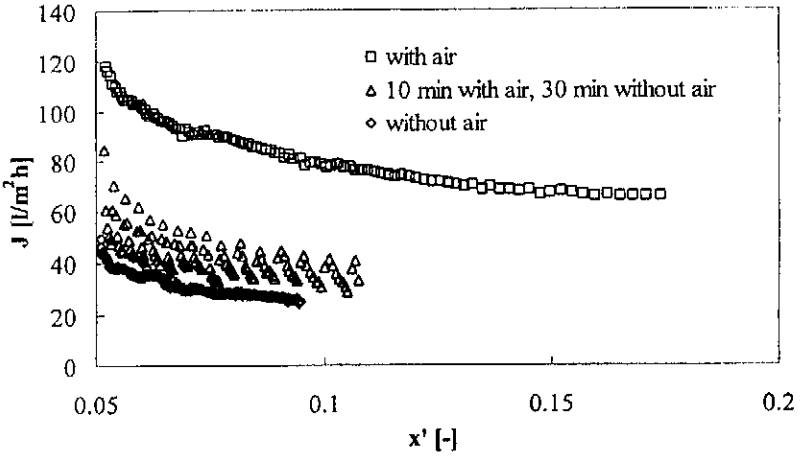

Fig. 7 Permeate flux vs. feed concentration during microfiltration of dispersion: $u = 1$ m s^{-1}, $\Delta P = 100$ kPa

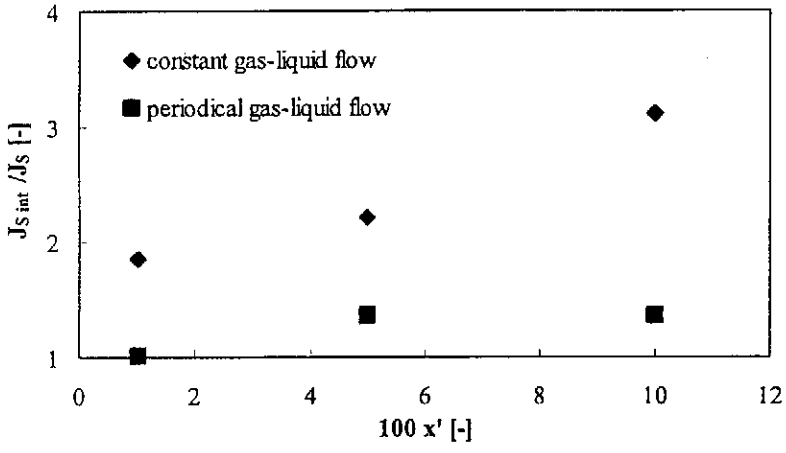

Fig. 8 Normalised steady state permeate flux as a function of the feed concentration: $u = 1$ m s^{-1}, $\Delta P = 100$ kPa

In the experiments using two-phase flow, air is injected throughout the filtering period. Here, there is also an initial flux decline but less important than the one observed without air. When the two-phase flow is constant, the flux is maintained at a higher level during the filtering period as shown in Fig. 7.

The most important consideration is that for all the concentrations in the range tested, an enhancement of the permeate flux is always observed because of the air injection. There is no concentration for which air injection has no effect on the flux.

To facilitate comparison between the three different systems considered the normalised permeate flux was plotted as a function of the solids mass fraction of the dispersions (see Fig. 8). The intensification effects of the constant gas-liquid two-phase flow were significant and for feed concentration 10 % wt. the flux was three times higher then fluxes without intensification. Lastly, a periodical gas-liquid flow seems to be less effective than a constant one in similar experimental operating conditions, even if it improves the flux in comparison with that without air.

Conclusion

The results of this experimental study demonstrated that in cross-flow microfiltration of dispersions, the gas-liquid two-phase flow could maintain the permeate flux at a constant and high level over the duration of an experiment.

The experiments carried out at a large number of flow conditions showed that the constant gas-liquid two-phase flow enhances microfiltration flux better than periodical gas flow. However, this phenomenon depends on the periodical gas flow mode and on the dispersion concentration. This effect is probably due to the high and transient wall shear stress induced by the gas flow. The hydrodynamic regime inducing the largest enhancement in flux is slug flow in the case of aqueous titania dispersion where a permeate flux plateau is reached at the beginning of the slug flow regime.

This process seems to be very promising, so further research and developments are under-way to optimise the process and to promote a better understanding of the mechanisms of deposit removal by gas-liquid two-phase flow.

Acknowledgements

The Grant Agency of the Czech Republic, Grant Project No. 104/00/0794, provided financial support for the research described.

Symbols

a particle radius, m
a_0 specific surface area, m^{-1}
c mass of solids deposited per volume of permeate, $kg\,m^{-3}$
J permeate flux, $l\,m^{-2}\,h^{-1}$
J_0 pure water permeate flux, $l\,m^{-2}\,h^{-1}$
J_s steady state permeate flux without intensification, $l\,m^{-2}\,h^{-1}$
$J_{s\,int}$ steady state permeate flux with intensification, $l\,m^{-2}\,h^{-1}$
k permeability, m^2
K Kozeny factor
K_1 constant, $s\,m^{-6}$
K_2 constant, $s\,m^{-3}$
ΔP transmembrane pressure difference, Pa
r cake layer resistance, m^{-2}
R_m membrane resistance, m^{-1}
S membrane area, m^2
t time, s
t_{ss} time predicted to achieve steady state, s
u liquid flow velocity, $m\,s^{-1}$
u_G gas flow velocity, $m\,s^{-1}$
V permeate volume, m^3
x' solids mass fraction

α specific cake resistance, $m\,kg^{-1}$
δ cake thickness, m
ε cake porosity
μ_l liquid viscosity, Pa s
ρ_s particle density, $kg\,m^{-3}$
τ_{cr} time constant, s
φ solids volume fraction
φ_{max} maximum solids volume fraction in the cake layer

References

[1] Mikulášek P.: Collect. Czech. Chem. Commun. **59**, 737 (1994).
[2] Cui Z.F., Wright K.I.T.: J. Membr. Sci. **117**, 109 (1996).
[3] Cui Z.F., Bellara S.R., Homewood P.: J. Membr. Sci. **128**, 83 (1997).
[4] Li Q.Y., Cui Z.F., Pepper D.S.: Chem. Eng. J. **67**, 71 (1997).
[5] Mercier M., Fonade C., Lafforgue-Delorme C.: Biotech. Techniq. **12**, 853 (1995).

[6] Mercier M., Fonade C., Lafforgue-Delorme C.: J. Membr. Sci. **128**, 103 (1997).
[7] Cabassud C., Laborie S., Lainé J.M.: J. Membr. Sci. **128**, 93 (1997).
[8] Laborie S., Cabassud C., Durand-Bourlier L., Lainé J.M.: Filtr. Sep. **34**, 887 (1997).
[9] Lee Ch.K., Chang W.G., Ju Y.H.: Biotech. Bioeng. **41**, 525 (1993).
[10] Davis R.H.: Sep. Purif. Methods **21**, 75 (1992).
[11] Bird R.B., Steward W.E., Lighfoot E.N., *Transport Phenomena*, Wiley, New York 1960.
[12] Mikulášek P., Wakeman R.J., Marchant J.Q.: Chem. Eng. J. **69**, 53 (1998).
[13] Mikulášek P., Doleček P.: Sep. Sci. Technol. **29**, 1183 (1994).
[14] Laborie S., Cabassud C., Durand-Bourlier L., Lainé J.M.: Chem. Eng. Sci. **54**, 5723 (1999).